

## Experimental characterization of the refrigerant distribution along a finned tubes heat exchanger

Luis Sánchez-Moreno-Giner\*, Emilio López-Juárez, Alejandro López-Navarro, José González-Maciá

Instituto Universitario de Investigación de Ingeniería Energética (IUIIE), Universitat Politècnica de València, València, 46022, Spain.  
e-mail: [luis.sanchez@iie.upv.es](mailto:luis.sanchez@iie.upv.es)

### ABSTRACT

According to the European Commission, heating, cooling and domestic hot water (DHW) production imply 79% of the total energy consumed in households. Moreover, as 84% of this energy is still generated from fossil fuels, it is required taking measures in order to improve the current situation.

Following this intention, the path of the European Union is the reduction of the energy consumption and increasing the percentage of energy produced by renewable sources. One way to achieve the objectives set by the European Union is by the use of the heat pump powered by renewable sources, while the directive 2009/28/CE consider that heat pumps use renewable sources under certain conditions.

Nowadays, refrigerants used by heat pumps are mainly hydrofluorocarbons (HFCs) which have a high global warming potential (GWP) and have a clear deadline defined at F-Gas EU Regulation 517/2014. For this reason, natural refrigerants, will play an important role within heating, cooling and DHW production at household sector. However, most of the natural refrigerants with acceptable thermodynamic properties are at least slightly flammable, and this attempt against the safety. For this reason, the amount of refrigerant charge must satisfy the maximum refrigerant charge limited by regulations, and the prediction of this maximum charge has become an important matter within the design process of a heat pump.

Nevertheless, calculating the amount of refrigerant for a given heat pump is a difficult process with many uncertainties, like refrigerant mal-distribution in heat exchangers.

In this work, an experimental characterization of the amount of refrigerant along the finned tubes heat exchanger (FTHE) of a heat pump working with R290 has been done. This qualitative and quantitative study has been carried out by measuring and comparing the temporary temperatures pattern distribution of the refrigerant in the FTHE, using thermocouples and thermographies

*Keywords: Refrigeration, refrigerant distribution, evaporator, refrigerant, thermography.*

---

### 1 Introduction

Due to the future lack of fossil fuels, the current energy consumption and its environmental impact such as the global warming and pollution; the society is in an energetical crisis.

The European Union has established energetic strategies to reduce the amount of global warming gas emissions, reduce the energy consumed and increase ratio of energy produced by renewable sources: Europe 2020 and Europe 2030 [1].

In the total energy consumed in Europe, the 40% is used in buildings [2] and 79% of the energy consumed in buildings is used for air conditioning and sanitary hot water production whilst for producing it, fossil fuels are majorly used (84%) [3].

One way to both increase the use of renewable sources and decrease the global warming gas emissions is by using heat pumps powered by renewable sources.

The problem is the global warming potential that the refrigerant gas has, i.e. the problems that would generate in case of leakage. Is for this reason that there is a regulation which limits the commercialisation of the refrigerants with high value of GWP and its use in new installations [4]. As a result of this regulation the price of the current refrigerants will rise, and a big number of alternatives are toxic or flammables. Thus, there is a growing importance on the refrigerant charge reduction and the total refrigerant charge estimation within any unit design process.

The number of studies concerning the topic of the refrigerant charge is increasing in the recent years. Examples of these studies are [5–7]. However, the studies about refrigerant charge estimation focus in the validity and precision of the different correlations of multiple phase flows [8] in the different part of the circuits, but there is little information about how maldistribution affects to an increase of the refrigerant charge needed.

In this contribution, it is presented an experimental study of the refrigerant behaviour in the FTHE used as an evaporator, comparing two cases with good and mal refrigerant distribution, and analysing its impact to the total refrigerant charge.

## 2 Methodology

The heat pump prototype has been tested in a climatic chamber able to control air temperature and humidity, simulating winter ambient temperatures. The climatic chamber is also equipped with an hydraulic loop, which simulates building heating demand by varying temperature and water mass flow. This used test rig is deeply detailed in a contribution from the CYTEF 2018 [9].

### 2.1 Test-rig

The heat pump prototype is a reversible air-to-water heat pump, *Figure 1* which uses R290 as refrigerant.

The heat pump has incorporated a rotary compressor with inverter technology to be able to modulate its heating capacity, following the standard UNE-EN-14825[10]. Additionally, it has a brazed plates heat exchanger (BPHE) working as a condenser, *Figure 1*, a FTHE as evaporator and a suction accumulator. This accumulator has the purpose of adjust the refrigerant charge needed in each condition and maintain superheat at the compressor inlet near 0K. Therefore, heating capacity is managed by an electronic expansion valve that controls subcooling instead of the usual superheat control.

*Table 2*, *Table 3* and *Table 4* show the characteristics of the components of the heat pump.

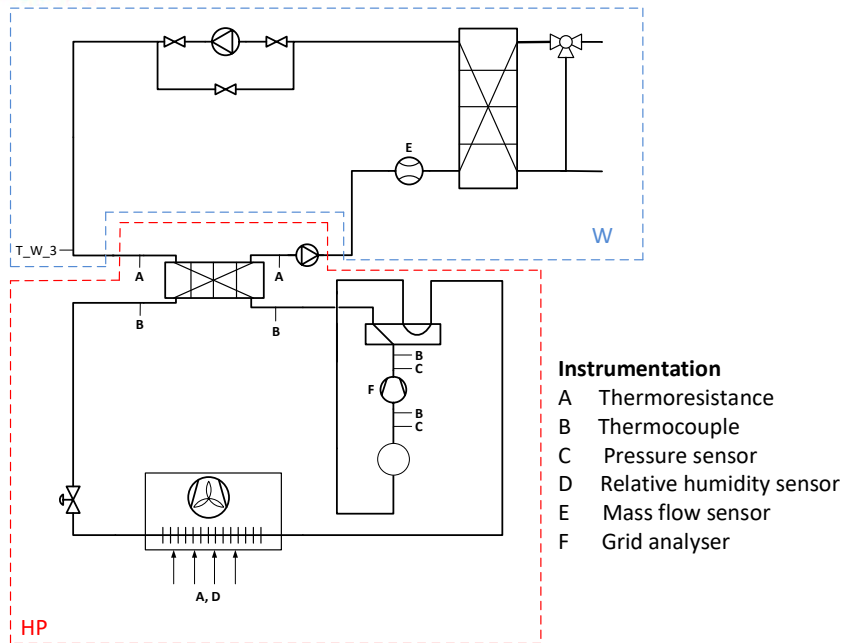


Figure 1: Test rig scheme.

	<b>Displacement cm<sup>3</sup></b>
<b>Compressor</b>	30.6

Table 1: Compressor characteristics.

	<b>Width mm</b>	<b>Height mm</b>	<b>Port Diameter mm</b>	<b>Plate Pitch mm</b>	<b>Number of plates</b>	<b>Flow type</b>
<b>BPHE</b>	72	329	24	1.1	34	Counter-current

Table 2: BPHE characteristics.

	<b>Tube diameter (mm)</b>	<b>Tube thickness (mm)</b>	<b>Inner surface</b>	<b>Transversal spacing (mm)</b>	<b>Longit. spacing</b>	<b>N. rows</b>	<b>N. circuits</b>	<b>Capillar inner diameter (mm)</b>
FTHE conf. 1	7	0.43	Rifflled	25	19	3	8	3.5
FTHE conf. 2	7	0.43	Rifflled	25	19	3	8	2

Table 3: FTHE configurations

<b>Refrigerant</b>	<b>Safety class</b>	<b>GWP<sub>100</sub>*</b>	<b>Critical temperature (°C)</b>	<b>Critical pressure (bar)</b>	<b>Heating volumetric capacity** (kJ/kg)</b>
<b>R290</b>	A3	3	96.7	4251.2	5.28

Table 4: Refrigerant characteristics.

\*GWP source: Regulation (EU) no 517/2014 of the European Parliament and of the Council [4]

\*\*Calculated with REFPROP [11] for condensation temperature of 35°C, evaporation temperature of 0°C, 5K of subcooling and 3K of superheat and isentropic efficiency of 100%.

To analyse the performance of the heat pump, the variables to be measured are selected following the standard UNE-EN-14511[12]. According to the standard as well, *Figure 12* shows thermocouples pattern distribution on each one of the eight circuits of the FTHE and *Table 5* shows uncertainties associated to each variable measurement.

Additionally, in order to understand in a deeper way refrigerant distribution at the FTHE, 56 thermocouples Class 1 [13] have been installed along each one of the eight circuits, and some thermographies have been taken front the frontal area of the heat exchanger (finned surface).

Thermographies has been taken with FLIR SC620 Infrared Camera with  $640 \times 480$  pixels, using qualitative analysis with surface emissivity 1 and distance 0.1 meters, due to this experimental analysis only has required a qualitative study in order to verify the battery thermal field. In this case, qualitative analysis is justified enough because only exists interest to know apparent temperatures along the battery, in order check if it is produced refrigerant mal-distribution at the FTHE. As *Figure 2* shows, in case of regular distribution the thermal field would follow a regular pattern of four tubes repeated eight times along FTHE height.

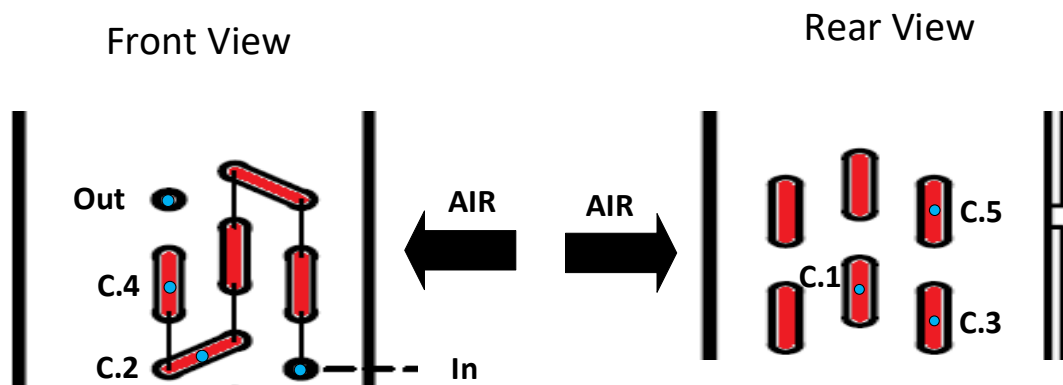


Figure 2: Thermocouple distribution on each one of the eight circuits of the FTHE.

Variable	Instrumentation	Resolution	Sensitivity	Uncertainty
Temperature	Thermocouple Class1	0.01°C	0.01°C	+0.5°C*
Temperature	FLIR SC620	640x480 pixels	0.065°C @30°C	+2% of Reading
Temperature	PT100 RTD	0.01°C	0.01°C	0.16°C
Pressure	PT5-30M	-	-	1.2 bar
Pressure	PT5-07M	-	-	0.16 bar
Mass flow	SITRANS F C MASS 2100 DI I5	-	-	5.2 kg/h
Humidity ratio	VAISALA HMP140A	0.01%	0.01%	3%
Power consumed	GOSSEN METRAWAT A2000	0.1W	0.1W	0.06kW

Table 5: Uncertainty of the instrumentation used.

## 2.2 Test plan

All the results have been obtained from stability periods of the tests A2W30 and A7W27 i.e. producing water at 30°C and 27°C having as air temperature 2°C and 7°C respectively. The stability is achieved where the principal variables' individual deviations are lower than 2.5% in case of the mass flow rates and 1K in case of temperatures or saturation temperatures.

These tests correspond to actual tests from experimental characterization campaign at partial loads. However, all the analysis are about specific moments and only data of a brief period of time from the whole test are being considered.

As mentioned the test conditions are two conditions of the campaign test according the standard UNE-EN-14825.

These two tests have been repeated with different refrigerant distributor of FTHE. More specifically, the configurations differ in the distributor of the heat exchanger, varying from the original and one with a lower inner diameter. With the change of the distributor the effect expected was helping to uniform the refrigerant distribution along the different circuits of the FTHE.

### 3 Results

As mentioned, there are two phases of results. The first phase is the initial heat pump with the distributor selected by the manufacturer. In this configuration two types of tests have been done: A7W27 and A2W30.

The main results can be seen in the *Table 6*.

Condition	Test	Heating Capacity kW	COP	Refrigerant mass flow kg/h
A7W27	Original distributor	3.42	5.10	35.11
A7W27	New distributor	3.59	5.30	35.90
A2W30	Original distributor	3.96	3.43	47.21
A2W30	New distributor	4.04	3.43	47.65

Table 6: Main results of the test performed.

The first study was done while performing the test of A7W27. During this test, no frost was produced in the evaporator but a block of ice was formed in the bottom part of the evaporator, *Figure 3*, and a difference of temperature in the different parts of the heat exchanger were seen. *Figure 4* shows can be seen the temperatures in the bends.



Figure 3: Block of ice in the bottom part of the evaporator.

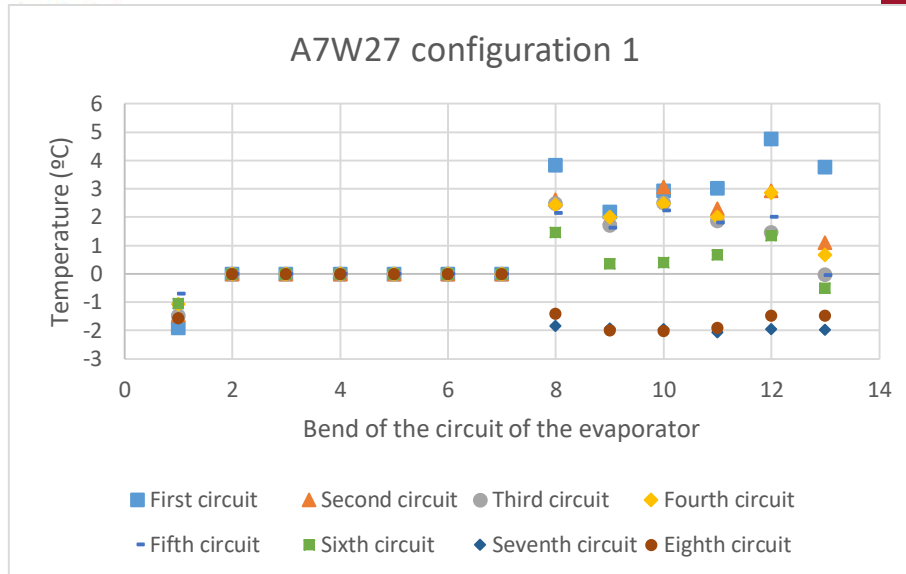


Figure 4: Temperature along the evaporator in the A7W27 test.

In *Figure 4* can be seen two different parts: the circuits with superheating and the circuits where any degree of superheating could not be observed. The part that corresponds with the non-superheated circuits is the bottom part of the heat exchanger, where the gravity makes more liquid or more refrigerant charge goes towards. Can be affirmed that in this test and in this configuration of the heat exchanger there is either a bad distribution of the refrigerant charge or a bad distribution of the phases of the refrigerant, going more quantity of the refrigerant through the last circuits or going through these circuits' refrigerant with lower quality.

Additionally, this effect can also be seen in the thermographic pictures, *Figure 5* and *Figure 6*, were taken at the same time that the data of the thermocouples.

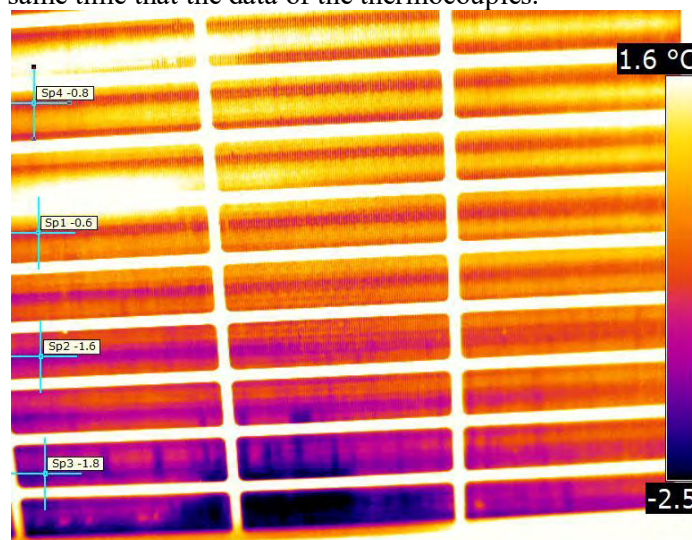


Figure 5: Thermographic picture of the block of ice in the bottom of the heat exchanger.

*Figure 5* shows the different map of temperatures of the evaporator and how the temperature decreases with the height. At the bottom of the figure can be observed the ice block previously mentioned and showed. The ice block was formed due to the condensation of the water in the air and when this water went down the fins, it has been frozen due to the temperature of the lower part of the wall of the evaporator.

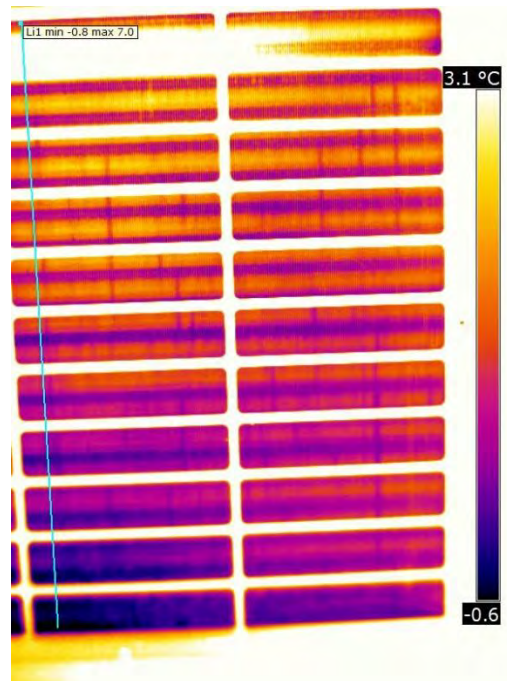


Figure 6: Thermographic turned picture of the evaporator. Top at left and bottom at right

Figure 6 shows the right half of the evaporator. Along the FTHE, a temperature difference can be seen. In the bottom part of the FTHE the refrigerant is still in saturation temperature while is not the case in the top of the heat exchanger. This effect is seen as a temperature difference of approximately 3K.

Figure 7 represents the temperature data of the values of the blue line at the left part in Figure 6:

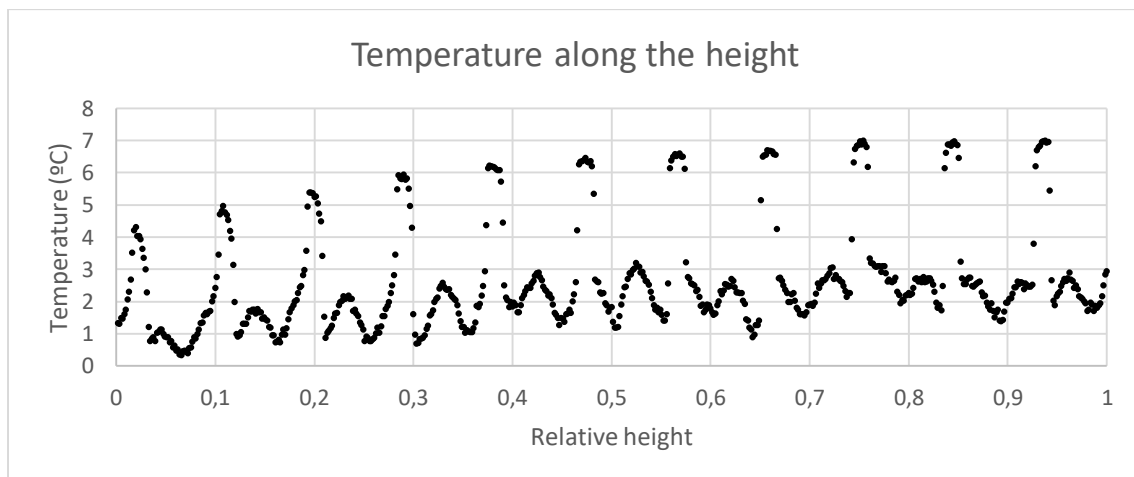


Figure 7: Temperatures along a vertical line of the evaporator.

In Figure 7 can perfectly be seen the decreasing trend of the temperature with the height, instead of seeing a regular patten distribution every four tubes. The discontinuities observed corresponds with the metal parts of the casing.

After the test A7W27 it was performed the test A2W30. This test is a transient test but for the purpose of the maldistribution of refrigerant study, a steady state period has been selected.

Figure 8 shows the temperatures in the bends of the heat exchanger for the test A2W30.

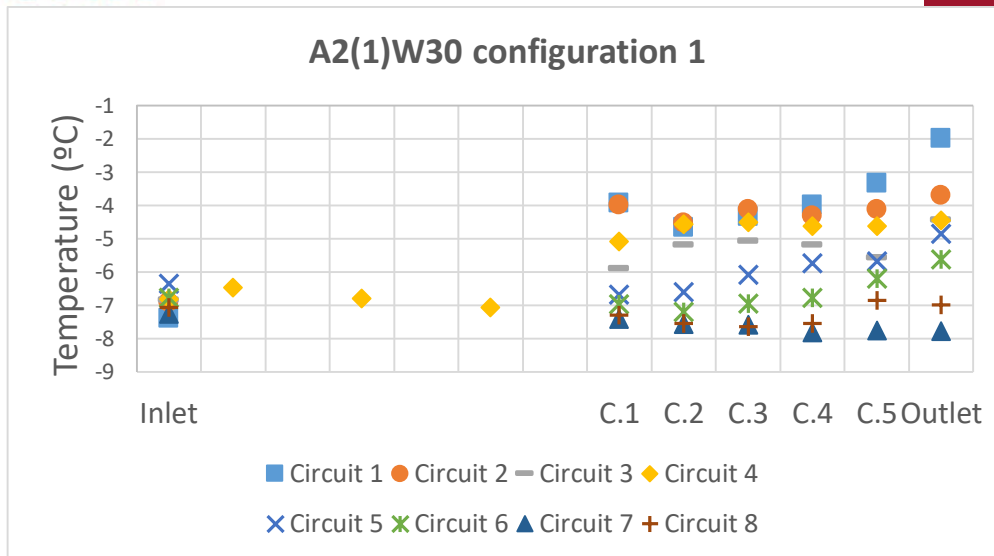


Figure 8: Temperature along the evaporator in the A2W30 test.

As it can be seen, the behaviour of the bad refrigerant distribution remains even though the increase of the mass flow of the evaporator. As happened in the A7W27 test, there are circuits with superheated gas and circuits without superheating (at the bottom part of the evaporator).

### 3.1 Distributor changed

After the discovery of the bad distribution, it was decided to change the distributor of the evaporator to another one with the capillary tubes with a smaller inner diameter. The aim of this was increasing the pressure drop in the capillary tubes to minimize the impact of the different pressure drop of the circuits of the evaporator.

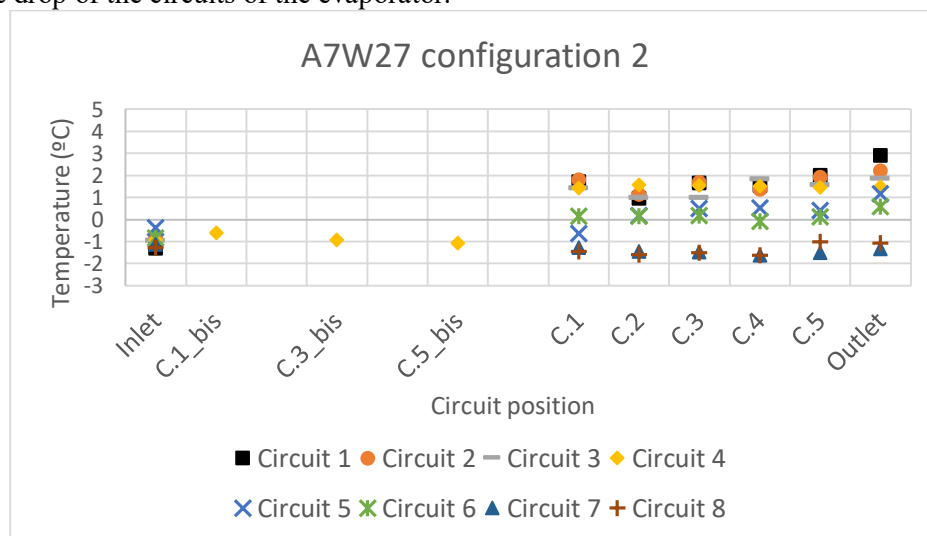


Figure 9: Temperature along the evaporator in the A7W27 test with the new distributor.

Figure 9 shows the different temperatures of the bends after the change of the distributor. There is a little difference between this case and the original one, there is still difference between the circuits but this difference has been reduced.

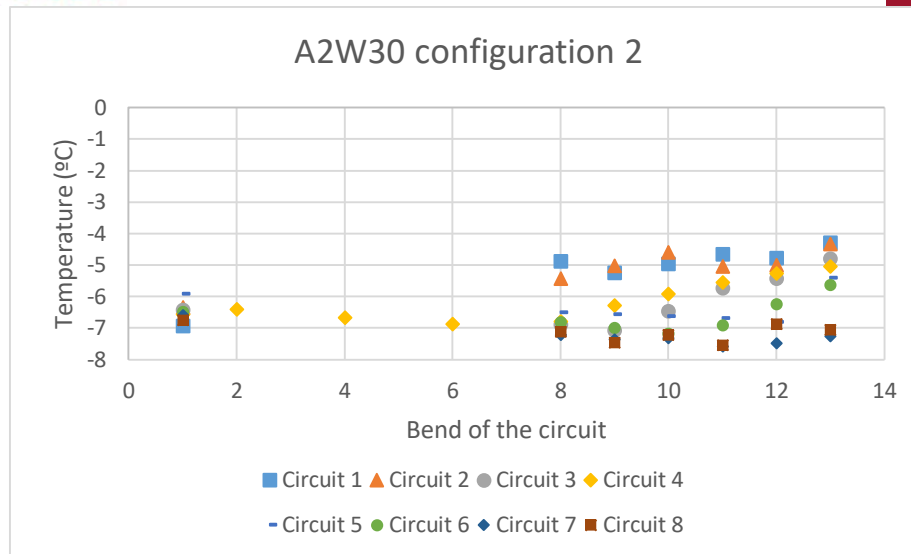


Figure 10: A2W30 with the new distributor.

On the other hand, comparing Figure 10 and Figure 8, the distribution has improved significantly. The dispersion between the circuits has been decreased but there is still difference and therefore maldistribution.

### 3.2 Analysis and discussion

The problem added to the maldistribution of refrigerant, apart from the deterioration of the performance, is the increase of the amount of refrigerant charge needed to behave similar to the same heat pump with perfect refrigerant distribution.

The effect of maldistribution can imply a difference of the refrigerant charge used. In order to analyse this effect, a model based on the experimental results has been done using the software IMST-ART.

In the model, each circuit of the evaporator has been divided in 59 cells, and in each cell the thermodynamic and transfer properties are calculated. In order to calculate the density of the refrigerant, as in the evaporator a phase change occurs, the thermophysical properties must be calculated according to these models. Thus, the density of the mixture of liquid and vapour is calculated following the equation (1).

$$\rho_m = \alpha \cdot \rho_V + (1 - \alpha) \cdot \rho_L \quad (1)$$

Where  $\alpha$  is the void fraction and is calculated with the Chisholm correlation [14] (2)

$$\alpha = 1 + \left[ \frac{0,8}{1 + \frac{21}{X_{tt}} + \frac{1}{X_{tt}^2}} \right]^{1.75} \quad (2)$$

Then with the density and the volume the charge estimation of each condition is easily done.

To calculate the density of each circuit it has been needed to use the quality inlet of the refrigerant in the circuit. These values have been estimated using the results of the experimental tests.

The model has been used to compare two different situations for the test conditions of A7W27. It has been considered the evaporation temperature of the test accomplished for the configuration 1 of the FTHE i.e. an evaporation temperature of  $-2^\circ\text{C}$ .

In *Table 1* can be seen the results obtained of the estimated refrigerant charge between the cases of ideal distribution and maldistribution in the FTHE.

Condition	FTHE configuration	Distribution model	Estimated charge (g)*
A7W27	Configuration 1	Maldistribution	118.30
A7W27	Configuration 1	Ideal distribution	39.76

Table 7: Difference between the estimated refrigerant charge.

As it can be seen the maldistribution affects negatively to the refrigerant charge even though that in the model there has not been the transient behaviour that has been observed during the experimental tests.

The maldistribution increases the charge of refrigerant due to the velocity difference between the liquid and vapour phases, while the mean quality of the gas is equal in the maldistribution model and ideal model, the mean void fraction of both models differs.

Additionally, in the experimental tests, it has been observed a difference of 40g in the refrigerant charge needed even though with the improvements the distribution was not near the ideal distribution.

#### 4 Conclusion

There is a growing importance in the use of heat pumps in households to produce heating, cooling and domestic hot water and due to the current regulations natural refrigerants will play an important role in the short-medium term.

In order to increase the safety and reduce expenses, it is convenient to take actions to reduce the refrigerant charge in the units.

In this paper has been studied experimentally a heat pump using propane as refrigerant and has been shown the bad behaviour of one of its components, the evaporator. This bad behaviour was provoked by a maldistribution of the refrigerant and has induced in a deterioration of the performance and an increase of the refrigerant charge in the system.

Part of the maldistribution has been eased by changing the distributor of the FTHE but there is still room until achieving the ideal distribution.

#### 5 Acknowledgements

Luis Sánchez-Moreno-Giner acknowledges the Research and Development Aid Program (PAID-01-17) of the Universitat Politècnica de València for receiving the Research Fellowship FPI-UPV-2017.

#### REFERENCES

- [1] EUROPEAN COMMISSION. *Energy Efficiency | Energy*. [accessed. 2019-02-04]. Available at: <https://ec.europa.eu/energy/en/topics/energy-efficiency>
- [2] ENERGY DG, E C. *EU energy in figures, statistical pocketbook*. 2017.
- [3] EUROPEAN COMMISSION. *Heating and cooling | Energy*. [accessed. 2019-02-04]. Available at: <https://ec.europa.eu/energy/en/topics/energy-efficiency/heating-and-cooling>
- [4] PARLAMENTO EUROPEO. *Reglamento (UE) nº 517/2014 sobre gases fluorados de efecto invernadero*. 2014, **2014**, 195–230.
- [5] FERNANDO, P; PALM, B; LUNDQVIST, P; GRANRYD, E. *Propane heat pump with low refrigerant charge: design and laboratory tests*. *International Journal of Refrigeration*. 2004, **27**(7), 761–773.
- [6] HRNJAK, P; LITCH, A D. *Microchannel heat exchangers for charge minimization in air-cooled ammonia condensers and chillers*. *International Journal of Refrigeration*. 2008, **31**(4), 658–668.

- [7] POGGI, F; MACCHI-TEJEDA, H; LEDUCQ, D; BONTEMPS, A. *Refrigerant charge in refrigerating systems and strategies of charge reduction. International Journal of Refrigeration*. 2008, **31**(3), 353–370.
- [8] THOME, J R. *Void Fractions in Two-Phase Flows*. 2004.
- [9] CORBERÁN, J M; MONTAGUD, C. *Initial Test Campaign of an Innovative Dual Source Heat Pump*. 2018, 19–21.
- [10] AENOR. *UNE-EN\_14825:2016*. 2016.
- [11] LEMMON, E W; MCLINDEN, O M. *NIST Reference Fluid Thermodynamic and Transport Properties — REFPROP. Database*. 2002.
- [12] AENOR. *UNE-EN\_14511:2014*. 2014.
- [13] AENOR. *UNE-EN\_60584-2 Termopares. Tolerancias*. 1996, **00**(91).
- [14] CHISHOLM, D. *Two-Phase Flow in Heat Exchangers and Pipelines. Heat Transfer Engineering*. 1985, **6**(2), 48–57.